Research Article

The Journal of Anatomy (ISSN 2995-6552)

# Effect of Alcohol and Wnt Signaling Pathway Interactions in Zebrafish (*Danio rerio*) Tooth Development.

**Parnia Azimian Zavareh[1], Sophie Chen[1], Devi Atukorallaya[1]*.**

Department of Oral Biology, Dr. Gerald Niznick College of Dentistry, Rady Faculty of Health Sciences, University of Manitoba, Winnipeg, Canada.

**Corresponding author**
Dr. Devi. Atukorallaya ,
Department of Oral Biology, Dr. Gerald Niznick College of Dentistry Rady Faculty of Health Sciences University of Manitoba Winnipeg, Manitoba, R3E0W2 Canada.
Tel : 1-204-789-3256
Fax : 1-204-789-3948
Email : devi.atukorallaya@umanitoba.ca

**Received Date :** September 23, 2024
**Accepted Date :** September 24, 2024
**Published Date :** October 26, 2024

**Running Title :** Alcohol –Wnt interactions in Tooth Development

## ABSTRACT

Alcohol consumption during pregnancy can negatively affect fetal development. Prenatal alcohol exposure (PAE) has been linked to various birth defects, including several dental anomalies commonly observed in individuals with Fetal Alcohol Spectrum Disorder (FASD), such as Decayed, Missing, and Filled Teeth (DMFT), malocclusion, caries, speech impairments, and enamel defects. While distinct developmental defects associated with PAE are well-documented, the underlying mechanisms leading to such phenotypes in tooth development remain poorly understood. One possible explanation is that alcohol may interfere with key signaling pathways involved in tooth development. In this study, we used zebrafish (Danio rerio) as a model to investigate how alcohol disrupts tooth morphology, histological arrangement, and cellular changes through its interaction with the Wnt signaling pathway. Zebrafish embryos were treated with 1% alcohol, 2mM LiCl (Wnt activator), 10nM WC-59 (Wnt inhibitor), and combinations of alcohol with the Wnt modulators. Whole-mount staining and histological analysis across experimental groups revealed differences in tooth and tooth germ numbers, size, shape, mineralization patterns, and Wnt10a and Wnt10b expression levels. Interestingly, the combined treatment of alcohol and LiCl resulted in phenotypes similar to alcohol exposure alone, while the combination of alcohol and WC-59 acted synergistically to further disrupt tooth development.

**Keywords :** Zebrafish; teeth; Fetal alcohol spectrum disorder; alcohol; Wnt signaling pathway.

## INTRODUCTION

Addictive substances are known to cause developmental defects when exposed to the fetus in utero (Meyyazhagan, Kuchi Bhotla et al. 2023). Ethanol (alcohol) is a widely consumed psychoactive substance whose societal prevalence can be attributed to its ease of production, cultural and social acceptance as a beverage, and traditional use (Ornoy and Ergaz 2010, Gupta, Gupta et al. 2016, Dangardt and Chikritzhs 2020). However, it is also a potent teratogen, capable of causing significant harm to fetal development. Alcohol consumption during pregnancy exposes the developing fetus to this teratogen, resulting in a range of birth defects (Silva, Azimian Zavareh et al. 2022). The first observations of fetal alcohol-related birth defects were made in 1968 by Lemoine et al., who identified a series of birth defects in 127 children exposed to alcohol prenatally (Lemoine, Harousseau et al. 2003). In 1973, Jones and Smith coined the term Fetal Alcohol Syndrome (FAS) to describe the constellation of birth defects resulting from prenatal alcohol exposure (PAE), including growth impairments, developmental delays, craniofacial dysmorphology, central nervous system abnormalities, and anomalies in the heart, limb, and kidneys (Jones, Smith et al. 1973, Da Silva and Wood 2021). Since then, additional morphological, organ-related, and cognitive defects have been linked to PAE. Specifically, individuals with Fetal Alcohol Spectrum Disorder (FASD) often present with a variety of oral abnormalities and dental deficits, including a high prevalence of Decayed, Missing, and Filled Teeth (DMFT), malocclusion, caries, speech impairments, and enamel defects (Blanck-Lubarsch, Dirksen et al. 2019).

Vertebrate tooth development involves intricate interactions between the epithelium and the underlying neural crest-derived mesenchyme. During this process, epithelial cells differentiate into ameloblasts, the enamel-secreting cells;

The Journal of Anatomy (ISSN 2995-6552)

while odontoblasts, which line the tooth pulp and are responsible for dentin formation, arise from the mesenchyme (2013). The primary regulatory mechanisms governing tooth development is dependent on communication between the epithelium and the mesenchyme, guiding key events such as epithelial placode formation and budding, mesenchyme condensation, and epithelial folding and growth – each essential for tooth morphogenesis (2013). These mechanisms are mediated by the secretion of signaling molecules and growth factors, namely the transforming growth factor beta (TGFβ), bone morphogenetic protein (BMP), fibroblast growth factor (FGF), hedgehog, and Wnt families (Thesleff 2006)Among these, the Wnt gene family is especially crucial for cell development and differentiation (Tamura and Nemoto 2016). Secreted as ligands, Wnt proteins activate downstream receptor-mediated pathways that play a pivotal role in the development of ectodermal appendages, such as teeth (Mikkola and Millar 2006, Liu, Chu et al. 2008). The canonical Wnt signaling pathway operates at multiple stages of tooth development and morphogenesis (Liu, Chu et al. 2008). Experimental manipulation of this pathway, through Wnt antagonists and agonists, has shown that Wnt pathway inhibition is associated with tooth anomalies, such as oligodontia, tooth agenesis, and crown and root dysmorphologies (Yang, Wang et al. 2015, Yuan, Zhao et al. 2017, Ruiz-Heiland, Lenz et al. 2019), while constitutive activation of this pathway leads to large, mishappen tooth buds and ectopic teeth (Liu, Chu et al. 2008). Many Wnt genes are expressed in the oral and dental epithelia, as well as in developing teeth (Liu, Chu et al. 2008), including Wnt4, Wnt5a, Wnt6, Wnt10a, Wnt10b, to name a few (Sarkar and Sharpe 1999). In particular, mutations in Wnt10a are linked to impaired tooth development, such as hypodontia, taurodontism, and ectodermal dysplasia syndromes (Yang, Wang et al. 2015, Yu, Liu et al. 2020). Furthermore, alterations in Wnt10a gene expression can influence other tooth development genes, suggesting that Wnt10a exerts both direct and indirect effects on tooth formation (Yuan, Zhao et al. 2017).

While tooth development is largely under genetic control, it is also subject to environmental influences. Research has shown that alcohol exposure can impact various stages of toothdevelopment, and animal studies have demonstrated that alcohol alters the basal layer of the tooth germ epithelium (inner enamel epithelium), reduces calcification of the dentin matrix, and delays eruption as well as cell differentiation in the tooth germ (Bowden, Weathersbee et al. 1983, Sant' Anna, Tosello et al. 2005, Sant'Anna, Tosello et al. 2005). Human studies on PAE have also highlighted dental alterations, malocclusions, agenesis, and twisted teeth (Church, Eldis et al. 1997). However, more research is needed to determine the prevalence and impact of dental caries and enamel defects in individuals exposed to alcohol in utero (Naidoo, Norval et al. 2006, Blanck-Lubarsch, Dirksen et al. 2019). In addition to its effects on odontogenic cells, alcohol exposure has also been shown to interfere with cell signaling, which may lead to cleft lip with or without cleft palate, or cleft palate only (Church, Eldis et al. 1997, Raterman, Metz et al. 2020). One of the mechanisms by which alcohol disrupts signaling is through the suppression of the Wnt pathway. Indeed, alcohol has been shown to reduce the expression of Wnt10a in the craniofacial region and around the pharyngeal cavity, further supporting its role in craniofacial abnormalities (Vangipuram and Lyman 2012).

While various craniofacial defects have been associated with PAE, and alcohol's detrimental effects on tooth development are evident in FASD, the underlying mechanisms remain largely unknown (Jones, Smith et al. 1973, Sant'Anna and Tosello 2006,Blanck-Lubarsch, Dirksen et al. 2019, Da Silva and Wood 2021).Given the complexities and limitations of human research on PAE, zebrafish have been adopted as a reliable animal model to better understand these processes (Eichler, Grunitz et al.2016, Fainsod and Hicks 2018, Almeida, Andreu-Fernández et al. 2020). Zebrafish (*Danio rerio*) have emerged as a popular and viable model organism in biological research, offering reproducible experiments with genetic and environmental control (Barkley-Levenson and Crabbe 2012, Kitson, Ord et al. 2022). Its unique advantages include rapid development,external fertilization, easy maintenance, and evolutionarily conserved alcohol-metabolizing genes (Reimers, Hahn et al.2004, Lovely, Fernandes et al. 2016, Fernandes, Buckley et al.2018). With 70% of their functional genes related to human diseases, zebrafish share both genetic and physiological similarities with humans (Barbazuk, Korf et al. 2000, Howe,Clark et al. 2013). Although zebrafish differ from mammals in terms of morphology and histology, their transparency and rapid embryonic development facilitate observation and experimentation (Lewis and Eisen 2003). Thus, zebrafish serve as an effective model to study human development, including the teratogenic effects of alcohol (Fernandes, Buckley et al.2018). Our lab has previously explored the impact of alcohol on zebrafish tooth development. Key findings demonstrated that embryonic alcohol exposure led to abnormal tooth formation, defects in palatal cartilage development and differentiation, and disruptions in melanocyte patterning,suggesting potential teratogenic effects of alcohol on neural crest-derived structures (Azimian Zavareh, Silva et al. 2022).

However, the mechanisms behind these phenotypic changes require further investigation as they may result either from alcohol-induced changes, interactions between alcohol and specific genes, or the activation/inhibition of complex cellular metabolic pathways (Azimian Zavareh, Silva et al. 2022). In the current study, we hypothesize that alcohol exposure during embryonic development and Wnt–alcohol interactions do

The Journal of Anatomy (ISSN 2995-6552)

lead to defects in tooth development. We aim to investigate the effects of alcohol and Wnt signaling pathway interactions on zebrafish tooth development at both the morphological and histological levels.

## MATERIALS AND METHODS

### Zebrafish Rearing and Breeding

Wild-type zebrafish (WT-AB) were kept under controlled water conditions regulated by the Tecniplast rack system at the Bannatyne campus, University of Manitoba. The zebrafish breeding colony was originally purchased from The Hospital for Sick Children (SickKids), University of Toronto. Fish were maintained following the established institutional guidelines. Adult zebrafish were fed a diet of Gemma 300–supplemented live shrimp and maintained on a 14/10 day/night cycle. Embryos were collected through natural spawning, transferred to clean Petri dishes containing embryo medium, and raised in an incubator at 28.5˚C for five days. At 5 days post fertilization (dpf), the embryos were transferred to the larval-rearing nursery tanks within the rack system.

### Alcohol and Wnt Pathway Modulator Treatment and Embryo Fixation

For this study, zebrafish embryos were treated with five different chemicals: 1% alcohol (Cat. No. HC13001GL, Fisher Scientific, USA), 2 mM Lithium chloride (LiCl, Cat. No. 866405-64-3, TCI, USA), 10 nM WC-59 (Cat. No. 500496, Sigma Aldrich, USA), and combined treatments of 1% alcohol with 2 mM LiCl and 1% alcohol with 10 nM WC-59 at the age of 10 hours post fertilization (hpf). Approximately 50 embryos were placed in Petri dishes containing each treatment solution. The concentrations selected were previously determined to be effective in fish research (Dlugos and Rabin 2003, Parsons, Trent Taylor et al. 2014). After 12 hours of exposure, the treatments were terminated, and the embryos were washed several times in fish rearing water before being raised according to standard operating procedures. At designated time points, embryos were euthanised using 1% tricaine methanesulphonate (MS222) (Cat. No. 118000500; Acros Organics, USA) and fixed overnight in 4% paraformaldehyde (PFA). The fixed embryos were then stored in phosphate-buffered saline (PBS) for subsequent analysis.

### Whole-Mount Double Staining

Acid-free double cartilage and bone staining was performed for tooth analysis, following standard Alcian blue and Alizarin red staining protocols (Walker and Kimmel 2007). Specimens were processed through an ascending series of glycerol in 1% KOH before being transferred to a 100% glycerol(Sadeghi, Amoli et al. 2015) storage solution (Sadeghi, Amoli et al. 2015). We examined 4 biological replicates (clutches) for each treatment (6) and each age (4) group. Each clutch contained n=12 embryos (range: 12-17). **Table 1** indicates the data for tooth length and width. The same fish were used to analyze tooth cusp morphology, cusp length, and cusp morphology.

**Table 1:** Samples size, mean tooth length and width measured with ZEN 2011 software in control and treated samples in 15, 20, 25, and 30 dpf. The samples were collected from 4 different clutches. Mean height of the tooth was measured by the maximum length from the tip of the tooth to the upper base of the tooth. Tooth width was measured from upper base to the lower base of the tooth.

| 15 dpf Samples | Sample Size | Mean of Tooth Length(µm) | Mean of Tooth Width(µm) |
|---|---|---|---|
| Control | 12 | 69.81 | 22.73 |
| 1% EtOH | 16 | 58.29 | 14.29 |
| 2m MLiCl | 16 | 71.89 | 25.49 |
| 1% EtOH +2m MLiCl | 16 | 54.35 | 17.48 |
| 10nMWC59 | 15 | 52.65 | 14.32 |
| 1% EtOH + 10nMWC59 | 16 | 40.09 | 13.54 |

| 20 dpf Samples | Sample Size | Mean of Tooth Length(µm) | Mean of Tooth Width(µm) |
|---|---|---|---|
| Control | 13 | 72.40 | 24.65 |
| 1% EtOH | 16 | 63.90 | 22.35 |
| 2m MLiCl | 17 | 78.50 | 28.17 |
| 1% EtOH +2m MLiCl | 17 | 61.42 | 19.12 |
| 10nMWC59 | 15 | 59.90 | 18.13 |
| 1% EtOH + 10nMWC59 | 15 | 55.25 | 19.27 |

| 25 dpf samples | Sample Size | Mean of Tooth Length(µm) | Mean of Tooth Width(µm) |
|---|---|---|---|
| Control | 12 | 90.85 | 29.18 |
| 1% EtOH | 17 | 91.43 | 30.17 |

The Journal of Anatomy (ISSN 2995-6552)

| | | | |
|---|---|---|---|
| 2m MLiCl | 17 | 100.57 | 39.86 |
| 1% EtOH +2m MLiCl | 16 | 67.57 | 23.87 |
| 10nMWC59 | 15 | 65.02 | 24.43 |
| 1% EtOH + 10nMWC59 | 15 | 63.02 | 22.86 |

| **30 dpf samples** | **Sample Size** | **Mean of Tooth Length(μm)** | **Mean of Tooth Width(μm)** |
|---|---|---|---|
| Control | 13 | 98.76 | 48.74 |
| 1% EtOH | 16 | 98.05 | 48.19 |
| 2m MLiCl | 17 | 122.63 | 48.22 |
| 1% EtOH +2m MLiCl | 17 | 77.94 | 32.69 |
| 10nMWC59 | 15 | 71.88 | 28.06 |
| 1% EtOH + 10nMWC59 | 16 | 69.90 | 27.17 |

**Electron Microscopy (EM)**

Zebrafish at 6 dpf (n= 6 per group) were treated with 1% alcohol, 2mM LiCl, 10nM WC-59, and 1% alcohol combined with 2mM LiCl or 10nM WC-59. After euthanasia, the fish were placed in 1.5 ml Eppendorf tubes and fixed in 3 % Glutaraldehyde in 0.1M Sorensen's buffer for 3 hours, ensuring that the fixative volume was 10 times greater than the tissue volume and that tissues remained free-floating. After fixation, the fixative was removed using a Pasteur pipette and replaced with 5 % Sucrose in 0.1M Sorensen's buffer for 1 hour. This solution was then replaced with fresh 5 % Sucrose in 0.1M Sorensen's buffer solution, and the fish samples were stored at 4°C. The protocol for preparing the thick section library was as follows: Tissues were post-fixed in Osmium tetroxide (OsO4), dehydrated in an ethanol series with a final methanol wash, and infiltrated briefly with propylene oxide. They were then embedded in resin (Embed 812) at room temperature and cured in a 60°C oven overnight. Blocks were stored at room temperature until needed. Sections of ~0.5-1μm were cut on a Reichert-Austria Om U3 Ultra-microtome with glass knives and collected on glass slides. These sections were stained with toluidine blue, washed with ethanol, cleared in xylene, and coverslipped.

Toluidine blue images of tooth morphology, degree of enameloid and dentin mineralization, and pulp cells of the functional tooth and tooth germs were assessed using High-definition Color Camera Head DS-Fi2 and Standalone Camera Control Unit DS-L3 (Nikon Eclipse E600, Japan). The same histological areas were further processed for the electron microscopy imaging. Histological processing was carried out by the Histomorphological and Ultrastructural Imaging Platform, Department of Human Anatomy and Cell Science, University of Manitoba.

**Wnt10a Immunofluorescence Protocol for Whole-Mount Staining of 10 dpf Zebrafish**

The above treated 10 dpf zebrafish (n = 6 per group) were processed for whole-mount immunofluorescence staining with Wnt10a antibodies according to standard protocol (Varatharasan, Croll et al. 2009). The following modifications were made: PBS was replaced with PBS-Tween (0.1 Tween 20) and stored at 4°C overnight. The samples were rinsed with distilled water for less than 1 minute and then fixed in acetone at -20°C for 20 minutes. After fixation, they were rinsed again with distilled water for 1 minute. The samples were transferred to 1% DMSO/1% TritonX in PBS (PBSDT) at room temperature (RT) overnight for permeabilization, allowing subsequent antibodies to infiltrate. After permeabilization, PBSDT was replaced with 5% Normal Goat Serum in PBSDT blocking solution for 1 hour. The experimental groups (positive control, alcohol, LiCl, WC-59, alcohol + LiCl, and alcohol + WC-59) were incubated with primary Wnt10a antibodies (1:1000 dilution in PBSDT) at 4°C for 5 days, while the negative control was kept in PBSDT without the primary antibody. The samples were then washed 8 times (approximately 15 minutes) with PBSDT and incubated with secondary Alexa 488 antibodies (1:800 dilution in PBSDT) for 3 days at 4°C on a shaker. Samples were washed with PBS-Tween for 15 minutes and stored in 35% glycerol in PBS-Tween at 4°C. All immunostained 10 dpf zebrafish samples were carefully exposed to the pharyngeal tooth-bearing regions using fine glass/tungsten needles. The samples were then observed in PBS-Tween on a fluorescence microscope using ZEN Microscopy Software.

**Whole-Mount In Situ Hybridisation (WMISH)**

Wnt10a and Wnt10b probes were prepared according to the manufacturer's instructions (DIG RNA Labeling kit, SP6/T7, Cat. No. 11175025910; Roche). Probe strength was detected via the dot blot technique. Briefly, 1 μl of diluted Wnt10a and Wnt10b probes was applied to a positively charged nitrocellulose membrane (Cat. No.11209299001; Roche). The membrane was placed in a glass container and incubated in a hybridization oven at 100˚C for 40 minutes. Next, it was soaked in 20 ml of maleic acid buffer for 2 minutes at room temperature on a shaker, then incubated in blocking buffer for 20 minutes on a shaker. The membrane was washed with TBST for 5 minutes on a shaker before being incubated with 10 ml of the antibody solution (Cat. No. 11093274910;

The Journal of Anatomy (ISSN 2995-6552)

Roche) for 30 minutes. The antibody solution was made by adding 2 µl of Anti-Digoxigenin antibody into 10 ml of TBST buffer. Following two washes with the washing buffer (15 minutes each), the membrane was incubated for 5 minutes in detection buffer. To detect the probe, 1 ml of BCIP/NBT liquid substrate solution (Cat. No.ICN980771; MP Biomedicals) was added on top of the membrane, which was kept in the dark and checked for a color reaction every 5 minutes. The reaction was stopped by adding TE buffer. The first dot was detected at the highest concentration within 5 - 10 minutes. (Erickson and Nicolson 2015)WMISH was performed on 48 hpf wild-type zebrafish embryos (n=6 per group) (Thisse and Thisse 2014).. After incubating in Hyb (-) solution, samples were exposed overnight to Wnt10a and Wnt10b probes in Hyb (+) solution at 70 °C. Colourimetric detection of RNA was performed using NBT/BCIP staining, and images were captured using a stereomicroscope in a 50% alcohol and 50% glycerol solution (Zeiss Discovery V8).

### Tooth Measurements

Zebrafish treated with the above alcohol and Wnt modulators were dissected using a Nikon-SMZ 10A dissecting microscope at 15, 20, 25, and 30 dpf to expose the lower pharyngeal jaw. Tooth count and measurements were performed following established protocols.

### Statistical Analysis

Data obtained were subjected to the independent T-test using Statistical Product and Service Solutions (SPSS) version 21. A P-value of < 0.05 was considered statistically significant. One-way ANOVA was conducted to assess treatment interactions, followed by Tukey's pairwise comparison to examine differences between treatments. A P-value of < 0.05 was also considered significant for Tukey's test. Furthermore, Chi-square analysis was performed to evaluate nominal data, such as tooth shape, with results considered statistically significant at $P<0.05$.

## RESULTS

### Tooth Mineralization Defects associated with Chemical Treatment

Zebrafish possess teeth on their 5th ceratobranchial arch (cb5), also known as their pharyngeal jaw. This bone holds three rows of teeth: the ventral (V), mediodorsal (MD) and dorsal (D) rows. In adult fish, the ventral row contains five teeth (1 V–5 V), the mediodorsal has four teeth (1 MD–4 MD), and the dorsal row contains two dorsal teeth (1 D–2 D) (**Supplementary Fig. 1A**). Mineralized pharyngeal teeth, attached to the bone, were stained dark red with alizarin red staining (**Supplementary Fig. 1A and 1B**). The alcohol-treated samples exhibited a reduction in alizarin red staining intensity at 15 and 20 dpf compared to the control (**Fig. 1E, F**), while the color intensity was similar at 25 and 30 dpf (**Fig. 1G, H**). This reduction in color intensity suggests that tooth mineralization was incomplete until 25 dpf. A similar reduction in staining was observed in LiCl-treated (**Fig. 1I, J**) and alcohol + LiCl-treated samples (**Fig. 1M, N**) at 15 and 20 dpf, indicating that tooth mineralization was also incomplete in these groups until 25 dpf. In WC-59-treated samples, reduced staining intensity was observed at 15, 20, and 25 dpf (**Fig. 1Q, R, S**), with tooth mineralization nearing completion at 30 dpf (**Fig. 1T**) compared to the control. In the alcohol + WC-59 treatment group, alizarin red staining was scarce and limited to the tips of the teeth at 15 and 20 dpf (**Fig. 1U, V**). By 25 dpf, tooth mineralization was observed in most teeth but was not fully completed at 30 dpf (**Fig. 1W, X**).

The Journal of Anatomy (ISSN 2995-6552)

**Figure 1**

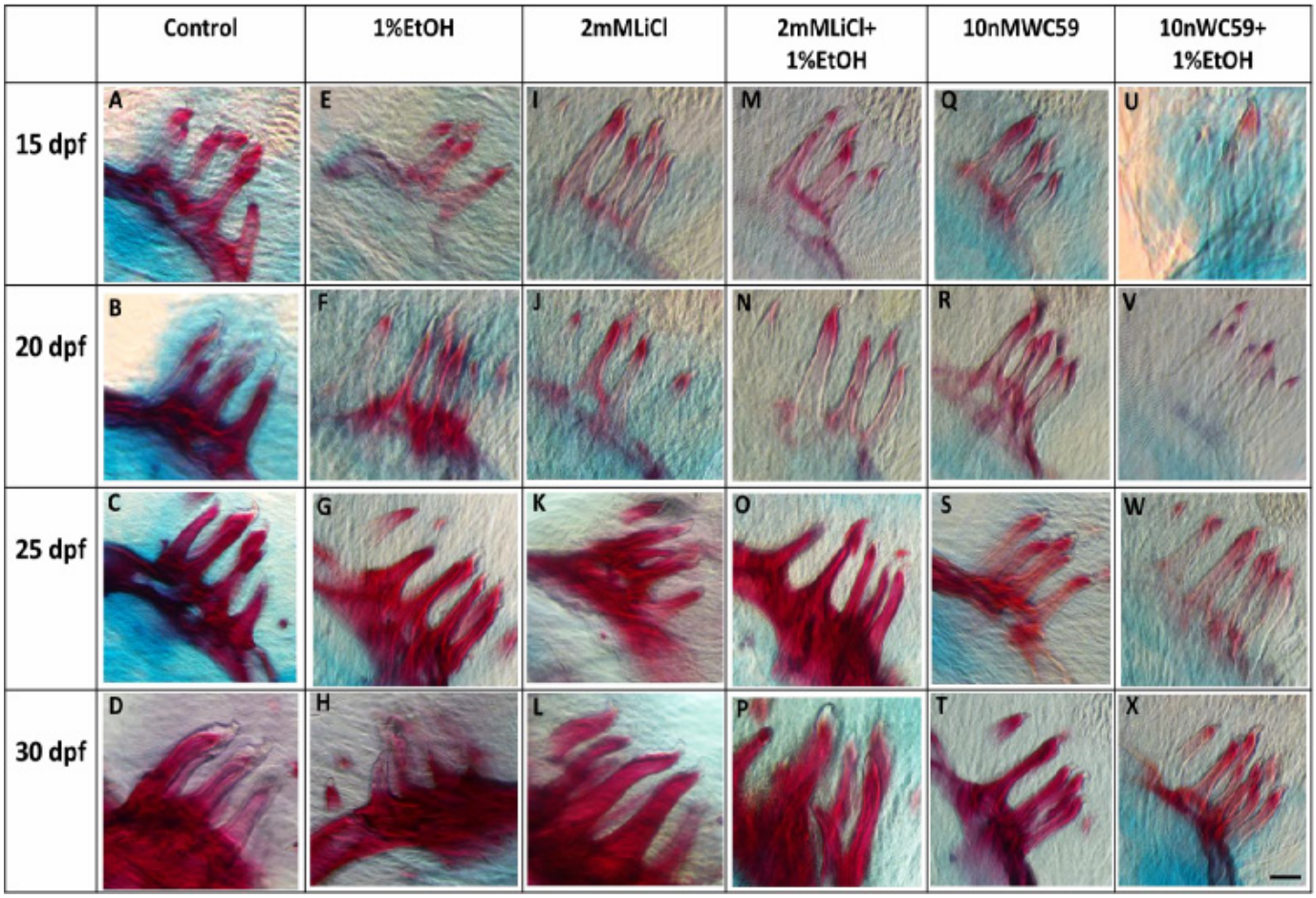


**Figure 1:** Acid-free double-stained tooth-bearing pharyngeal bones in zebrafish at 15, 20, 25, and 30 dpf. (A-D) Control samples showing lower pharyngeal bones with six fully mineralized, unicuspid teeth directly attached to the underlying bone. (E–H) Samples exposed to 1% alcohol, (I-L) 2mM LiCl, (M-P) 1% alcohol + 2mM LiCl, (Q-T) 10nM WC-59, and (U-X) 1% alcohol + 10nM WC-59 at 10 hpf exhibiting malformed and hypomineralized teeth. Scale bar: 20 µm.

**Tooth Number Alteration with Chemical Treatment**

The sample groups imaged in (**Fig. 1**) were used for the following analysis. By counting the attached teeth in acid-free double-stained sections of the pharyngeal jaw at each time point, we found that alcohol-treated samples had significantly fewer teeth than the control at 15 dpf (**Fig. 2**). Hypodontia was observed in alcohol-treated samples at 15 dpf, while tooth numbers at 20, 25, and 30 dpf (**Fig. 2**) were similar to the control. In the LiCl treatment group, an increase in tooth number was observed at 25 dpf, while this parameter was significantly lower than the control at 15 and 20 dpf (**Fig. 2**), suggesting that LiCl may regulate tooth number. The alcohol + LiCl treatment group showed a significant decrease in tooth number compared to the control at 30 dpf, but no significant differences were observed at 15, 20 and 25 dpf (**Fig. 2**). Notably, WC-59 treatment resulted in a significant reduction in tooth number at 25 and 30 dpf (**Fig. 2**), while the alcohol + WC-59 group exhibited decreased tooth numbers at all time points compared to the control, making it the most severely affected (**Fig. 2**). The tooth length, width and tooth cusp length data can be found in the (**Supplementary Fig. 2-9**).

The Journal of Anatomy (ISSN 2995-6552)

**Figure 2**

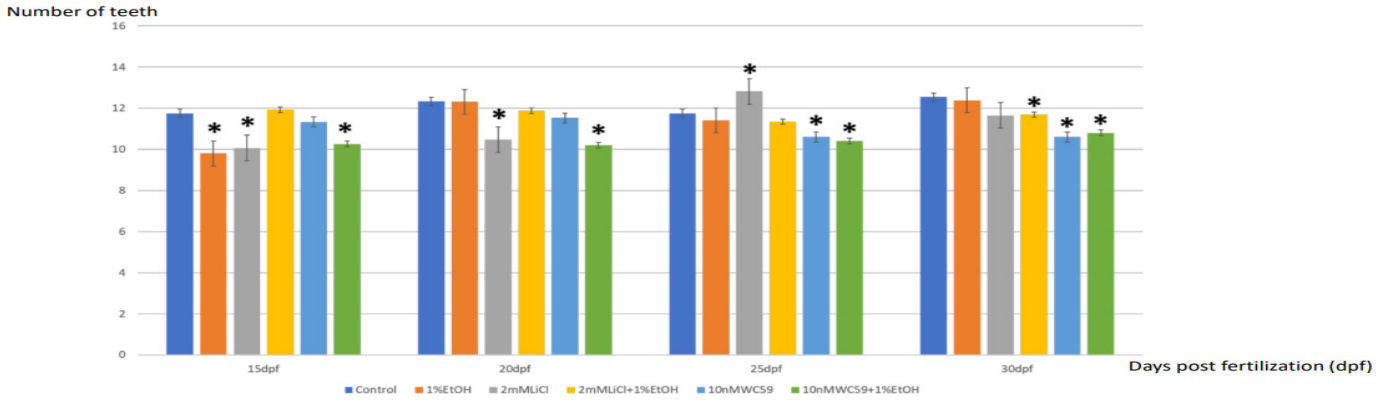


**Figure 2:** Comparison of tooth number between the control and chemically treated samples at 15, 20, 25, and 30 dpf. Asterisks indicate P<0.05. Attached tooth numbers were counted in the acid-free double-stained slides of the pharyngeal jaw at each time point (white arrowheads in Supplementary Figure 1A). In alcohol-treated samples, tooth number was significantly lower than the control at 15 dpf, but similar to the control at 20, 25 and 30 dpf. The LiCl-treated group showed a significant increase in tooth number at 25 dpf but was significantly lower than the control at 15 and 20 dpf. The combination of alcohol and LiCl resulted in a significant decrease in tooth number at 30 dpf, but not at 15, 20 or 25 dpf. In the WC-59 (Wnt inhibitor) treatment group, tooth number was significantly reduced at 25 and 30 dpf. The combination of alcohol and WC-59 significantly decreased tooth number at all time points compared to the control. Blue –control, Orange – alcohol-treated, Gray – LiCl-treated, Yellow – WC-59-treated, Light blue – alcohol + LiCl-treated, Green – alcohol+ WC-59-treated.

### Histological Analysis of Functional Teeth

Erupted functional teeth in zebrafish are directly attached to the 5th ceratobranchial arch (**Supplementary Fig. 1C**). The hard tissues and pulp in the different experimental groups were visualized using toluidine blue stain, which has a high affinity for acidic tissue components and glycosaminoglycans in mineralized tissues (Sridharan and Shankar 2012) (Sridharan and Shankar 2012). Compared to the control (0-1 vacuoles) (**Fig. 3 A**), all treatment groups exhibited a larger pulp with increased vacuoles (> 1 vacuoles). Changes in tooth size, shape, and stain intensity of hard tissues were also observed across the groups. Alcohol-treated samples showed lighter staining at the cusp tips (**Fig. 3B**). In the LiCl group (**Fig. 3C**), the stain intensity in the functional tooth was comparable to the control, though a wider and longer pulp with increased vacuoles as well as a change in tooth shape can be appreciated. When LiCl was combined with alcohol (**Fig. 3D**), however, the functional tooth increased in size but retained a similar shape to the control. In WC-59-treated samples (**Fig. 3E**), the staining was less intense at the cusp tip. Combining WC-59 with alcohol (**Fig. 3F, white dashed box**) significantly altered and blunted the tooth shape, with a marked decrease in stain intensity in the hard tissues. In all the chemically treated groups, mineralization was disrupted, resulting in either a thin enameloid collar or an overall reduced staining in hard tissues. More notably, attachment of the teeth to bone was interrupted in some cases (**Fig. 3B, C, D, F**).

**Figure 3:** Toluidine blue-stained cross sections of functional teeth (white-dotted rectangle) and tooth germs (yellow circle) of zebrafish at 6 dpf.

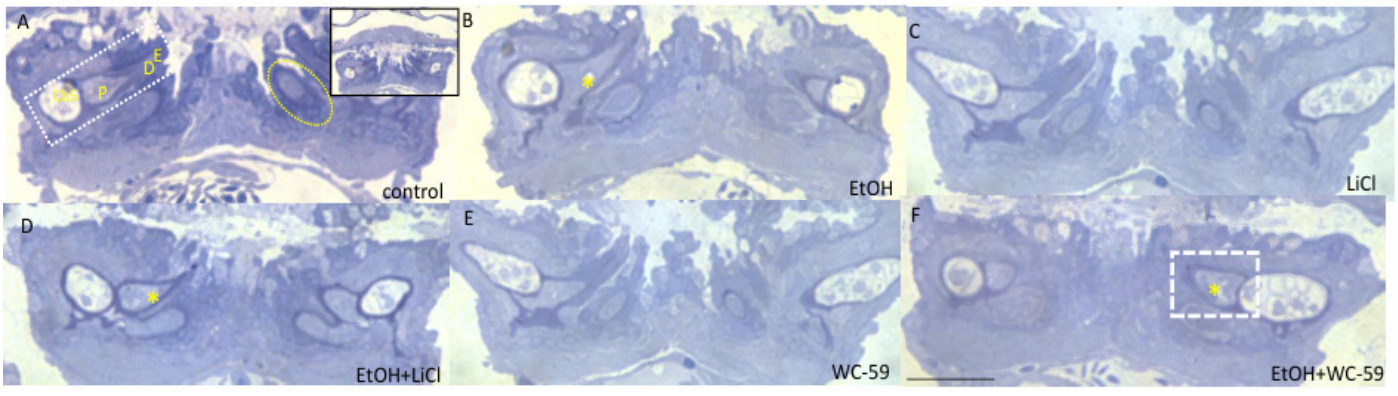


(A) Control samples showing minimal vacuole spaces in the pulp and high intensity staining in the hard tissues. Samples exposed to (B) 1% alcohol, (C) 2mM LiCl, (D) 1% alcohol + 2mM LiCl (E) 10nM WC-59, (F) 1% alcohol + 10nM WC-59 show alterations in pulp density, tooth size and shape, and stain intensity in hard tissues. White dashed box highlights a small, short tooth. Cb5: 5th ceratobranchial bone, P: pulp, D: dentin, E: enameloid. Yellow asterisk marks vacuoles/matrix vesicles in pulp cavities in B, D, and F. Scale bar: 1000 nm.

The Journal of Anatomy (ISSN 2995-6552)

**Histological Analysis of EM Images**

Analysis of tooth germs using electron microscopy revealed the hard tissue mineralization patterns and layers. In the untreated control fish samples, tooth germs showed a double layer of epithelial cells surrounding the dental papilla (**Fig. 4A, dark blue circles Tg1 and Tg2**). At higher magnification, electron micrographs revealed a high-density mineralization front with an intense, mineralized outer enameloid, measuring 2.72 µm thick (**Fig. 4C**, yellow double arrow). This mineralized front exhibited a layered appearance of predentin (**Fig. 4C**, red arrow), with a regular mineral deposition pattern. Alcohol-treated samples displayed a similar likeness under light microscopy, though with a reduced tooth germ length of 8 nm compared to 11 nm in the control. Contrarily, the dental papillae were larger, and tooth germs were more numerous in alcohol-treated samples (n=5) compared to the control (n=4) (**Fig. 4B**). EM images showed a thicker mineralization front (3.36 µm) of moderate density (**Fig. 4D**). However, the predentin's layered appearance was lost. A notable finding of LiCl-treated samples was increased proliferation and disorganization of epithelial cells, with a higher count of tooth germs (n=6) of comparable size (7.6 nm) to the control (6 nm) (**Fig. 4E**). This disorganized pattern was also seen in the 6.18 µm thick mineralization front (**Fig. 4G**), with a denser peripheral mineralization and a thinner predentin in the innermost layer. In alcohol + LiCl-treated samples, epithelial proliferation and tooth germ size were similarly increased (8.7 nm compared to 6 nm in controls) (**Fig. 4F**), with the electron micrograph showing a thicker mineralization front of 3.36 µm (**Fig. 4H**). However, tooth germ numbers remained similar to the control (n=4) (**Fig. 4F**). WC-59-treated samples had tooth germs that were scattered, smaller, and more numerous (n=7) (**Fig. 4I**). Electron microscopy revealed a dense enameloid periphery and a large, low-density mineralization front (2.9 µm) (**Fig. 4K**). Consistently showing the most significant changes, the combined alcohol and WC-59 treatment led to considerably smaller tooth germs with a single layer of epithelial cells surrounding the dental papilla. Epithelial proliferation was also disrupted, leading to scattered cells and a higher apparent tooth germ count (n=4) (**Fig. 4J**). Furthermore, the innermost predentin layer around the pulp was the thinnest among all groups (2.6 µm). Within the low-density mineralization front, an irregular mineralization pattern with few protein particles and a lower density enameloid periphery can be observed (**Fig. 4L**).

**Figure 4:** Toluidine blue-stained cross sections of tooth germs and corresponding electron micrographs of individual tooth germs of zebrafish at 6 dpf.

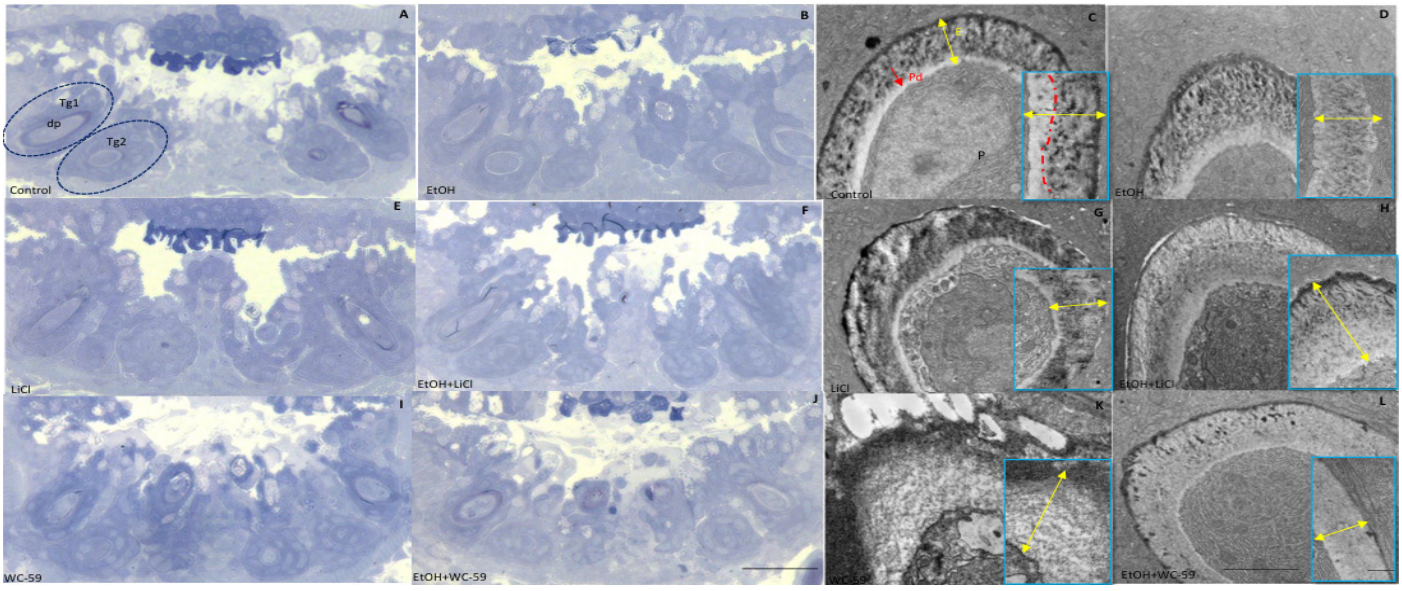


(A, C) Control sample showing a double layer of epithelial cells surrounding the dental papilla, with a high-density mineralization front and a highly mineralized outer enameloid (Blue dashed circles indicating two tooth germs Tg1 and Tg2). The electron micrograph of the individual tooth germ reveals the dental papilla surrounded by the mineralizing enameloid. The inlets in C, D, G, H, K, and L show enlarged views of the mineralization front of the tooth germ, focusing on the mineralized tissues, enameloid and predentin. Samples exposed to (B, D) 1% alcohol, (E, G) 2mM LiCl, (F, H) 1% alcohol + 2mM LiCl, (I, K) 10nM WC-59, (J, L) 1% alcohol + 10nM WC-59 show alterations in epithelial cell organization, tooth germ size and numbers, and changes in mineralization pattern and density in hard tissues. Tg1: Tooth germ 1, Tg2: Tooth germ 2, dp: dental papilla, E: enameloid, p: pulp, Pd: predentin. Double-headed arrows mark the mineralization front. Red arrows indicate the predentin layer. Red dashed lined indicate the margin of mineralization. Scale bar: 1000 nm (toluidine blue), 6 µm (EM).

The Journal of Anatomy (ISSN 2995-6552)

**The mRNA Expression of Wnt10a and Wnt10b**

Wnt10a and Wnt10b expression, indicated by purple colouration, was observed in the developing craniofacial region and pharyngeal cavity of 48 hpf larvae (**Fig. 5**). The negative control sample, which lacked the Wnt10a and Wnt10b probes, showed no such colouration (**Fig. 5A**). Notably, the LiCl-treated sample exhibited increased expression (**Fig. 5F, G**), while the other treatments resulted in a reduction, highlighting the impact of these treatments on Wnt signaling genes in the context of tooth development (**Fig. 5B, C, D, E, H, I, J, K, L, M**).

**Figure 5:** Ventral view of the whole-mount in situ hybridization of 48 hpf zebrafish, showing Wnt10a and Wnt10b expression in craniofacial regions.

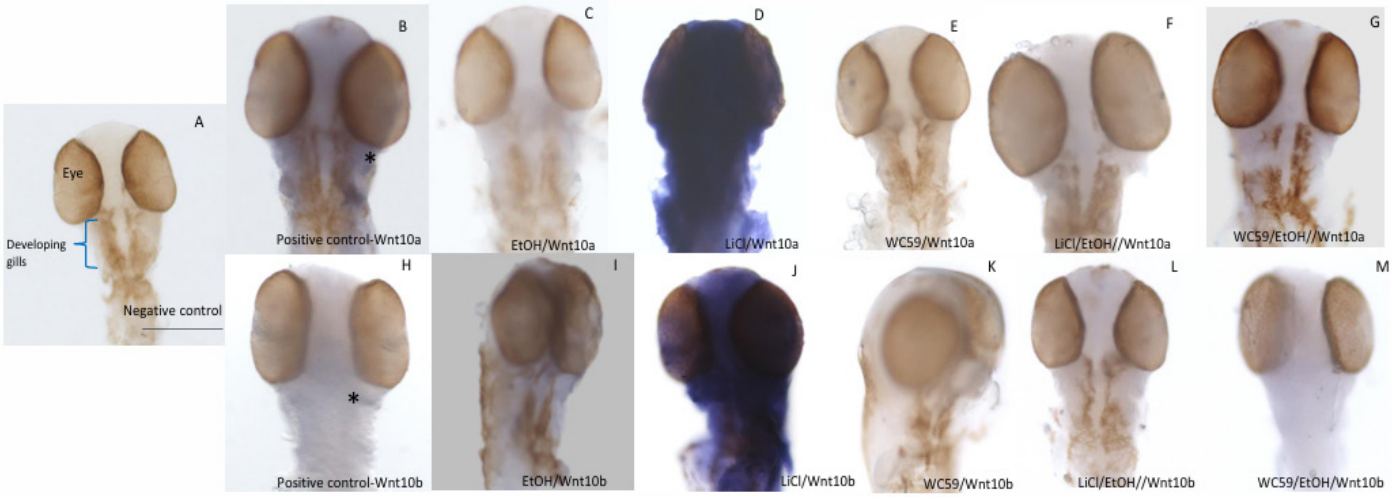


(A) Negative control, (B, C, D, E, F, G) Wnt10a probe expression. (H, I, J, K, L, M) Wnt10b probe expression, (B, C) positive control, (D, E) 1% alcohol, (F, G) 2mM LiCl, (H, I) 10nM WC-59, (J, K) 1% alcohol + 2mM LiCl, (L, M) 1% alcohol + 10nM WC-59. Blue brackets indicate the developing gills, and asterisks mark the tooth-forming region of the gill. E: eye. Scale bars: 50 μm.

**Analysis of Wnt10a Protein Expression in 10 dpf Zebrafish**

All treatment groups, excluding the negative control, which served as the baseline fluorescence (**Fig. 6A**), were incubated with Wnt10a antibodies and showed varying degrees of fluorescence intensity. The positive control exhibited fluorescent tooth-bearing regions and pharyngeal bones (**Fig. 6B**). The fluorescence was strongly increased in the LiCl-treated sample, displaying the most intense fluorescence of all treatment groups (**Fig. 6D**). In contrast, the other treatment groups showed either reduced or similar fluorescence intensity compared to the negative control (**Fig. 6 C, E, F, G**).

The Journal of Anatomy (ISSN 2995-6552)

**Figure 6:** Whole-mount immunohistochemistry of 10 dpf zebrafish using Wnt10a antibody, with the pharyngeal region dissected for better visualization.

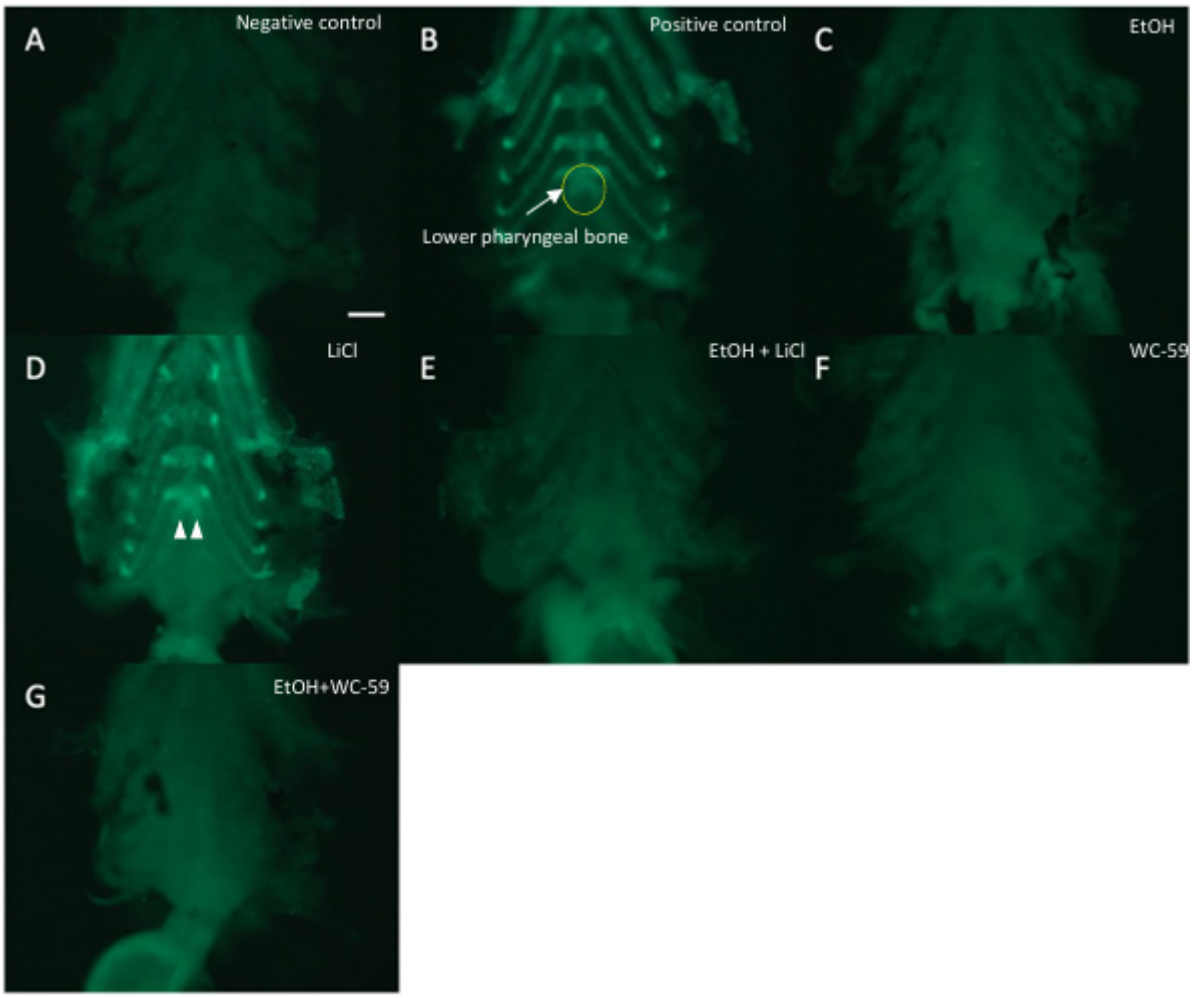


(A) Negative control, showing no Wnt10a expression in the pharyngeal tooth-bearing region. (B) Positive control, exhibiting bright florescence in the tooth-bearing bones (yellow circle) and cartilaginous gill joints (yellow arrows) of the gill rakers. (C) 1% alcohol, showing minimal Wnt10a expression. (D) 2mM LiCl, resulting in increased expression compared to both the negative and alcohol groups, with higher expression than the control. (E) 1% alcohol + 2mM LiCl, (F) 10nM WC-59, (G) 1% alcohol + 10nM WC-59, all showing minimal Wnt10a expression White arrowheads indicate pharyngeal bone with teeth. Scale bar: 50 µm.

## DISCUSSION

PAE has detrimental effects on various organs and body systems, including teeth (Mikkola and Millar 2006, Azimian Zavareh, Silva et al. 2022.) Although the mechanisms leading to the various tooth anomalies are not fully understood, it has been hypothesized that alcohol may directly or indirectly affect cells by interacting with signaling pathways crucial for tooth development (Azimian Zavareh, Silva et al. 2022) In this study, we utilized zebrafish treated with alcohol, LiCl (Wnt activator), WC-59 (Wnt inhibitor), and combinations of alcohol with the Wnt modulators to investigate the mechanisms by which alcohol interacts with the Wnt signaling pathway to cause the tooth defects observed in individuals with PAE.

Whole-mount staining of alcohol-treated groups revealed a reduced stain intensity of alizarin red (Fig. 1 E-H) and toluidine blue (Fig. 3 B), indicating a decrease in the production of calcium and glycosaminoglycans, to which alizarin red and toluidine blue bind, respectively (Walker and Kimmel 2007, Sridharan and Shankar 2012). Our results also showed a lower-density mineralization front in developing tooth germs (Fig. 4D) and a delayed point of complete mineralization at 25 dpf (Fig. 1E-H). Contrarily, untreated zebrafish samples initiated mineralization in their first pair of teeth at 82 hpf and achieved full mineralization by 4-6 dpf (Huysseune and Sire 1998, Huysseune and Sire 2004, Jackman, Draper et al. 2004). Notably, these observations are consistent with the existing literature documenting the negative impact of in vivo PAE on ameloblast secretory function and dentin matrix formation (Sant'Anna and Tosello 2006, Blanck-Lubarsch, Dirksen et al. 2019). Therefore, we can infer that alcohol

The Journal of Anatomy (ISSN 2995-6552)

has an inhibitory effect on tooth mineralization, thereby delaying and reducing the overall degree of mineralization in functional teeth. Consequently, this inhibition may disrupt their attachment to the pharyngeal bone (Fig. 3B, C, D, F), which correlates with early tooth exfoliation (Azimian Zavareh, Silva et al. 2022).Additionally, alcohol exposure appears to reduce the size of tooth germs and functional teeth. Our previous study reported that alcohol-treated samples exhibited straight tooth cusps with decreased tooth height and width (Azimian Zavareh, Silva et al. 2022).

Similarly, the tooth numbers at 15 dpf were also reduced (Fig. 2), but the return to normal levels at subsequent time points (Fig. 2) supports the hypothesis that adverse effects of alcohol are most pronounced in first-generation teeth and diminish over successive tooth replacement cycles (Erickson and Nicolson 2015, Atukorala and Ratnayake 2021).

The Wnt signaling pathway is of particular importance in early tooth development, and mutations in this pathway can lead to various tooth anomalies (Yang, Wang et al. 2015, Yuan, Zhao et al. 2017, Ruiz-Heiland, Lenz et al. 2019). Indeed, our experimentation with WC-59 showed a stronger inhibitory effect than alcohol alone. We observed a greater reduction in mineralization (Fig. 3E) and a delay in functional tooth mineralization, only beginning to attain complete mineralization at 30 dpf (Fig. 1Q-T). Additionally, the developing tooth germ displayed a thick mineralization front with very low density (Fig. 4K), suggesting that WC-59 may suppress ameloblast secretion. Interestingly, histological analysis of all chemically treated groups revealed enlarged pulps (Fig. 3), which may provide insight into our previous finding of a reduced cusp length-to-tooth length ratio in WC-59-treated samples. Notably, hypodontia at 25 dpf and 30 dpf (Fig. 2) and differences in tooth length and width overtime suggest that the inhibitory effects of WC-59 become more pronounced with successive tooth replacement cycles. In contrast, LiCl treatment led to an overall increase in cellular activity and Wnt gene expression (Fig. 5F, G, Fig. 6 D). Continuous activation of the Wnt signaling pathway resulted in disordered proliferation of epithelial cells (Fig. 4E), consistent with Handrigan et al.'s observation that canonical Wnt signaling promotes dental epithelial cell proliferation and tooth replacement in snakes (Handrigan and Richman 2010). Furthermore, a gradual increase in tooth number to hyperdontia at 25dpf in LiCl-treated samples (Fig. 2) is consistent with a study that observed an eruption delay in multiple teeth after treating cichlid embryos with LiCl (Fraser, Bloomquist et al. 2013). Interestingly, while LiCl functional teeth also displayed enlarged pulps (Fig. 3C), the cusp length-to-tooth length ratio was increased, indicating that the longer teeth were in fact due to increased cusp length. Indeed, EM analysis of LiCl-treated tooth germs revealed a haphazard, high-density mineralization front and a significantly denser enameloid periphery (Fig. 4G). Thus, we can infer that LiCl acts as an activator by stimulating epithelial and odontoblast-like cells, thereby augmenting enameloid secretion. Previous studies have highlighted the role of Wnt signaling in regulating dentin thickness, with Wnt10b specifically involved in odontoblast differentiation and expression of noncollagenous dentin proteins (Yamashiro, Zheng et al. 2007, Lim, Liu et al. 2014, Vogel, Read et al. 2016)

Our results from the combined alcohol and Wnt modulator treatments suggest that there is an interaction between alcohol and the Wnt signaling pathway in PAE tooth development. Given the inhibitory effects of alcohol and the activating effects of LiCl, one would expect the combined treatment to produce an intermediate outcome. However, the alcohol + LiCl-treated samples resembled those of the alcohol-only group. This manifestation may be explained by alcohol's role in increasing Tyr phosphorylation of GSK3b, which promotes the degradation of β-catenin, a key downstream protein in the Wnt signaling pathway (Vangipuram and Lyman 2012). Additionally, chronic high-dose alcohol exposure has been shown to inhibit Wnt signaling (Xu, de la Monte et al. 2015). Indeed, the Wnt10a and Wnt10b expression levels were significantly reduced (Fig. 5 J, K, Fig. 6 E). Similarly, alcohol + LiCl-treated tooth germs exhibited a shared likeness with the alcohol-only group (Fig. 4B, F) but with a lower density mineralization front (Fig. 4 H), further disrupting tooth mineralization (Fig. 1M-P). The functional tooth number and cusp shape were affected in later tooth replacement cycles in alcohol + LiCl samples compared to the early presentation in alcohol-treated samples (Fig. 2), which explains the relatively larger, yet normally shaped teeth (Fig. 3D). It is contradicting, however, that the tooth length and width have previously been observed to be increasingly less than the control at all time points.

In the alcohol + WC-59 treatment group, these parameters were consistently reduced, contrasting with the dominant effect of alcohol in the alcohol + LiCl group. Alcohol combined with WC-59 appears to exert a synergistic inhibitory effect on zebrafish teeth and developing tooth germs, resulting in more severe developmental defects than either treatment alone. We observed severe hypodontia and hypomineralization at all time points (Fig. 2, Fig 1U-X). Histologically, irregular epithelial organization (Fig. 4J) and abnormal mineralization patterns (Fig. 4 L) were noted. EM analysis revealed not only a consistently thin predentin around the pulp, but also a low-density mineralization front with hypomineralized enameloid (Fig. 4L), further indicating suppressed ameloblast secretion. These findings may imply that the combined inhibition from alcohol and Wnt signaling pathway interaction interferes with both dentin and enameloid formation. In fact, previous studies have shown that Wnt10b is primarily localized to the inner dental epithelium during the late bell stage (Nadiri,

The Journal of Anatomy (ISSN 2995-6552)

Kuchler-Bopp et al. 2004) Furthermore, histological examination revealed distorted cusps and pulps in functional teeth (Fig. 3F), as well as reduced cusp length-to-tooth length ratios. Misshapen teeth, such as these, have been identified as a common adverse effect of PAE (Whitehurst 2010).

## CONCLUSION

Based on our findings and in conjunction with previous studies, we conclude that alcohol may interact with the Wnt signaling pathway to contribute to the dental anomalies observed in PAE. Interestingly, alcohol exerts a strong inhibitory effect that can counteract the activating effects of LiCl, while alcohol and WC-59 appear to act synergistically to disrupt tooth development. Our EM analyses were limited by low magnification; thus, future studies using higher magnification would provide more detailed visualization of odontogenic processes and the collagen matrix, allowing for a better understanding of the temporal and spatial aspects of tooth development and its associated gene expression.

**Key findings**

1. Tooth development, such as tooth number and mineralization pattern, was stimulated by Wnt agonist LiCl and inhibited by alcohol, Wnt antagonist WC-59, and combined treatments.
2. Alcohol and Wnt modulators altered the shapes and sizes of functional teeth and developing tooth germs.
3. Alcohol may neutralize the activating effects of LiCl on Wnt expression and synergistically enhance the inhibitory effects of WC-59 on Wnt expression.

**Author contributions:** DA planned the study, assisted with interpreting the results, and revised and finalized the manuscript. PA conducted the chemical treatment and analysis the bone stained and insitu hybridization data. SC conducted the histological analysis, EM and immunofluorescence drafted and revised the manuscript.

**Acknowledgements:** This study was partially funded by the Natural Sciences and Engineering Research Council, Canada (NSERC) in the form of a NSERC Discovery grant RGPIN 05364-2019 to DA. SC was supported by the BSc dent program at the Dr. Gerald Niznick College of Dentistry. We acknowledge the University of Manitoba for supporting the Atukorale lab.

**Conflicting interest:** The authors have no conflicting interests.

**Supplemental Figure 1**. Acid-Free Double Staining Of 30 Dpf Zebrafish Dentition, Alizarin Red-Stained Tooth, And Histological Section Of The Toluidine Blue-Stained 6dpf Pharyngeal Region.

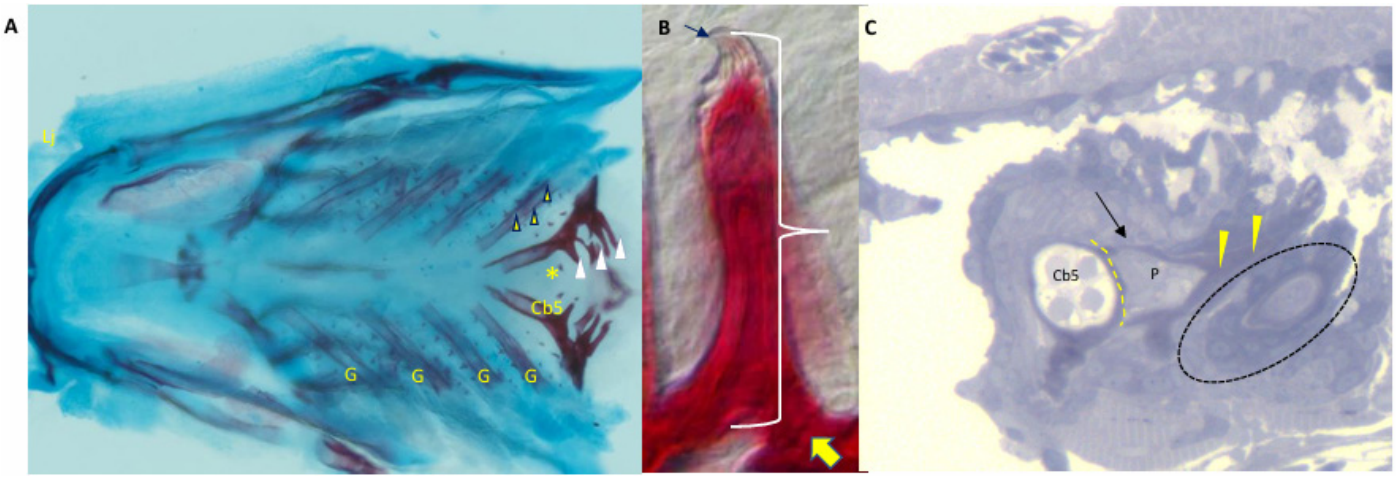


(A) Pharyngeal jaws oriented with the dorsal side facing up and the rostral side facing left, with red-stained pharyngeal gills, bones, and teeth. Attached functional teeth are marked with white arrowheads, exfoliated teeth are indicated by yellow asterisks, and the gill rakers are marked by yellow arrowheads. (B) Functional tooth attached to the underlying bone. Yellow arrow marks the tooth-bone attachment junction, and the bracket encompasses the functional tooth. The black arrow points to the cusp. (C) A cross section of the left 5th ceratobranchial bone attached to one functional tooth beside one developing tooth germ (circled). The black arrow indicates the functional tooth. The yellow dashed line denotes the tooth attachment site. The tooth exhibits a light-colored pulp in the center, covered by an inner dentin layer and an outer darker-stained enameloid layer (yellow arrowhead). Cb5: 5th ceratobranchial bone, P:pulp.

The Journal of Anatomy (ISSN 2995-6552)

**Supplemental Figure 2.** Comparing the tooth (A) length and (B) width in control and treated samples at 15 days post-fertilisation. There is a significant difference between the treated groups with the control in both tooth length and width ($P < 0.05$).

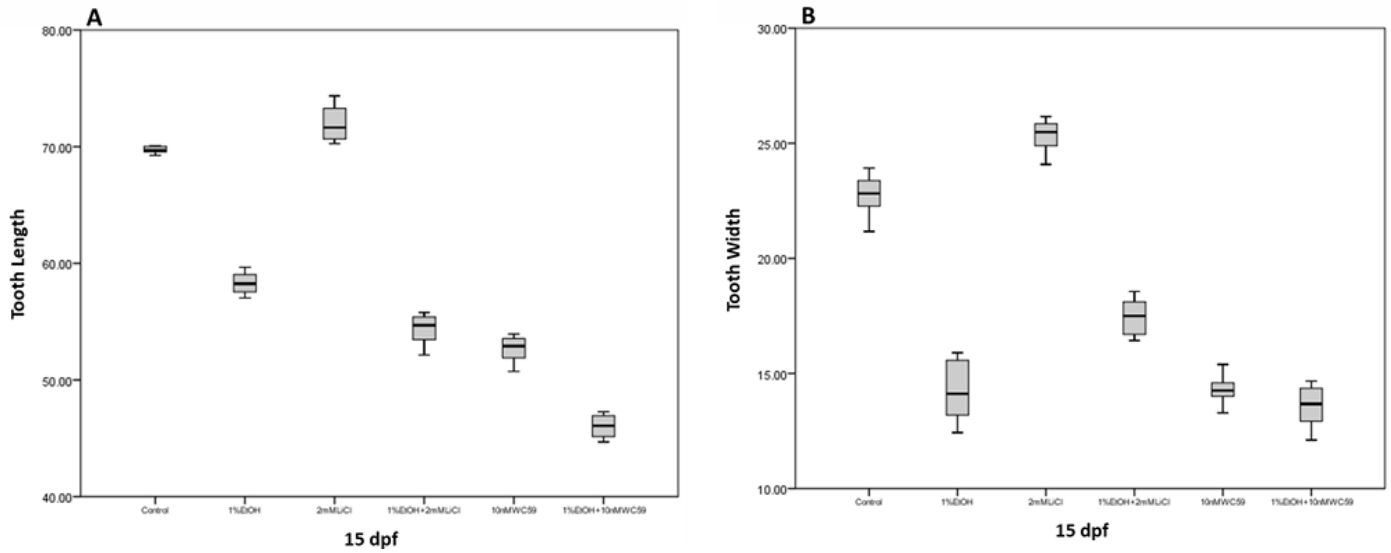


**Supplemental Figure 3.** Comparing the tooth (A) length and (B) width in control and treated samples at 20 days post-fertilisation. There is a significant difference between the treated groups with the control in both tooth length and width ($P < 0.05$).

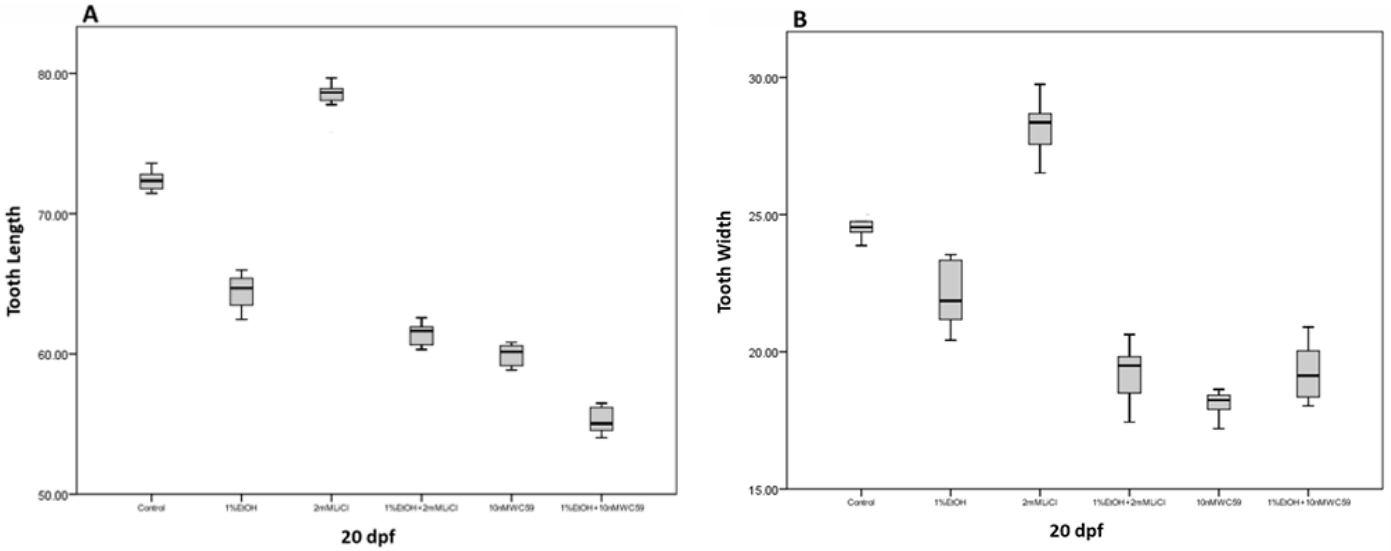

The Journal of Anatomy (ISSN 2995-6552)

**Supplemental Figure 4.** Comparing the tooth (A) length and (B) width in control and treated samples at 25 days post-fertilisation. There is a significant difference in tooth length and width between the 2mMLiCl, 1%EtOH+2mMLiCl, 10nMWC59, and 1%EtOH+10nMWC59 treated groups with the control ($P < 0.05$), while there was no significant difference between 1%EtOH treated samples with the control ($P > 0.05$).

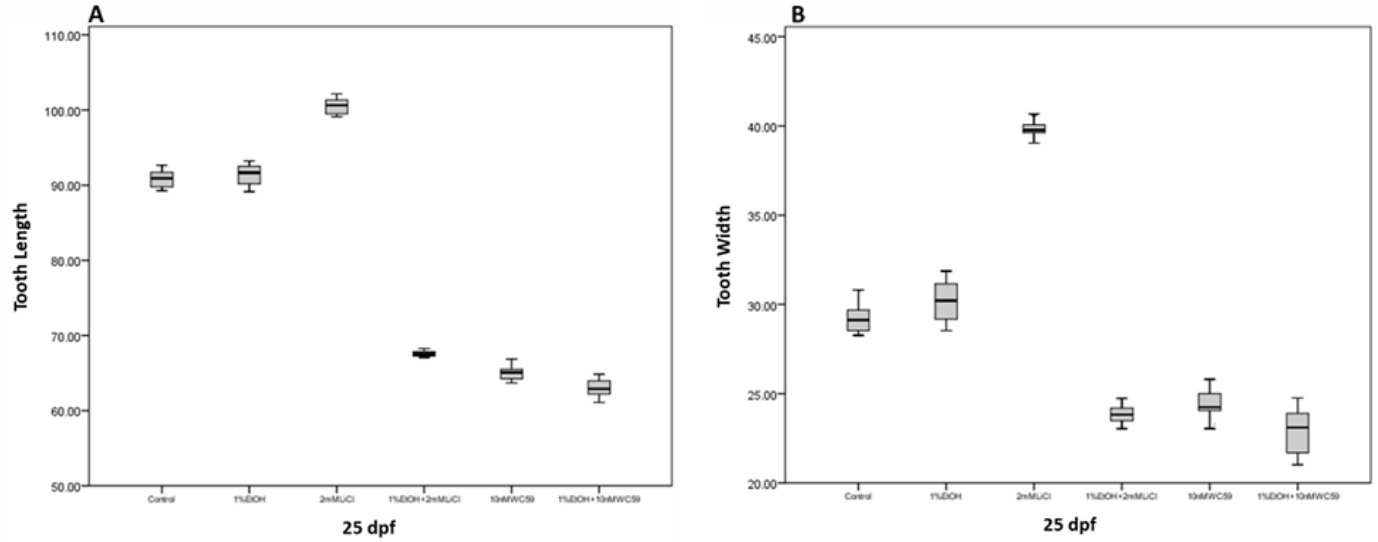


**Supplemental Figure 5.** Comparing the tooth (A) length and (B) width in control and treated samples at 30 days post-fertilisation. There is a significant difference in tooth length between the 2mMLiCl, 1%EtOH+2mMLiCl, 10nMWC59, and 1%EtOH+10nMWC59 treated groups with the control ($P < 0.05$), while there was no significant difference between 1%EtOH treated samples with the control ($P > 0.05$). There is a significant difference in tooth width between the 1%EtOH+2mMLiCl, 10nMWC59, and 1%EtOH+10nMWC59 treated groups with the control ($P < 0.05$), while there was no significant difference between 1%EtOH and 2mMLiCl treated samples with the control ($P > 0.05$).

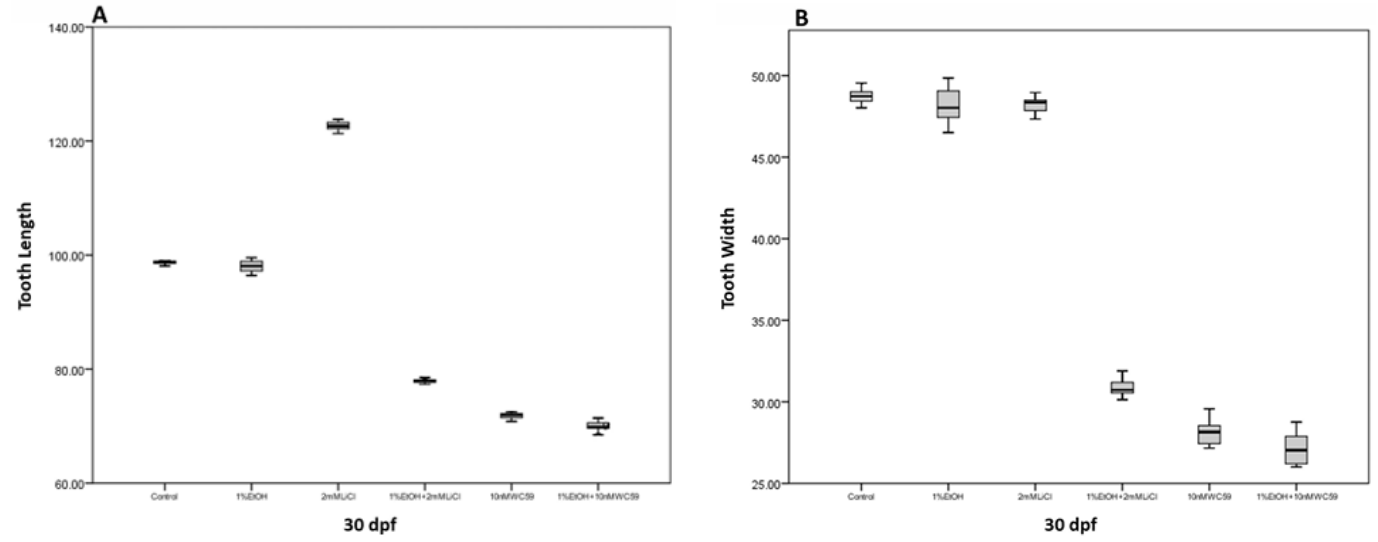

The Journal of Anatomy (ISSN 2995-6552)

**Supplemental Figure 6.** Comparing the cusp length between control and treated samples at 15 dpf. There was a significant difference in cusp length between the 1%EtOH, 2mMLiCl, 1%EtOH+2mMLiCl, 10nMWC59, and 1%EtOH+10nMWC59 treated groups with the control ($P < 0.05$).

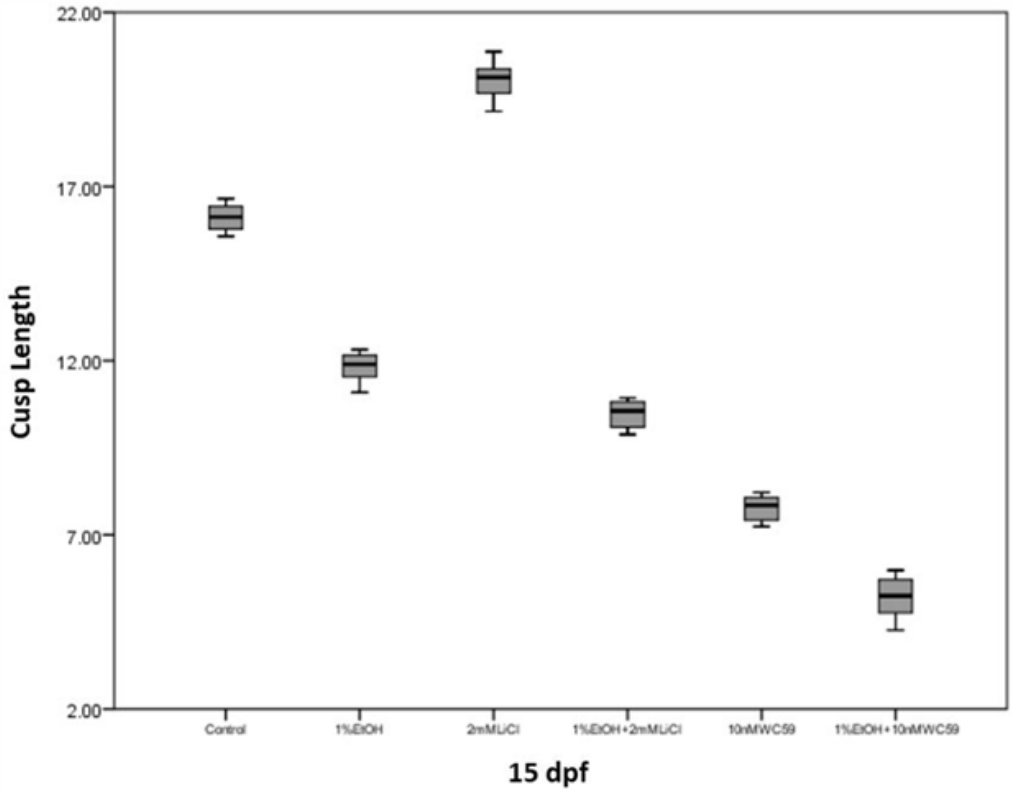


**Supplemental Figure 7.** Comparing the cusp length between control and treated samples at 20 dpf. There was a significant difference in cusp length between the 1%EtOH, 2mMLiCl, 1%EtOH+2mMLiCl, 10nMWC59, and 1%EtOH+10nMWC59 treated groups with the control ($P < 0.05$).

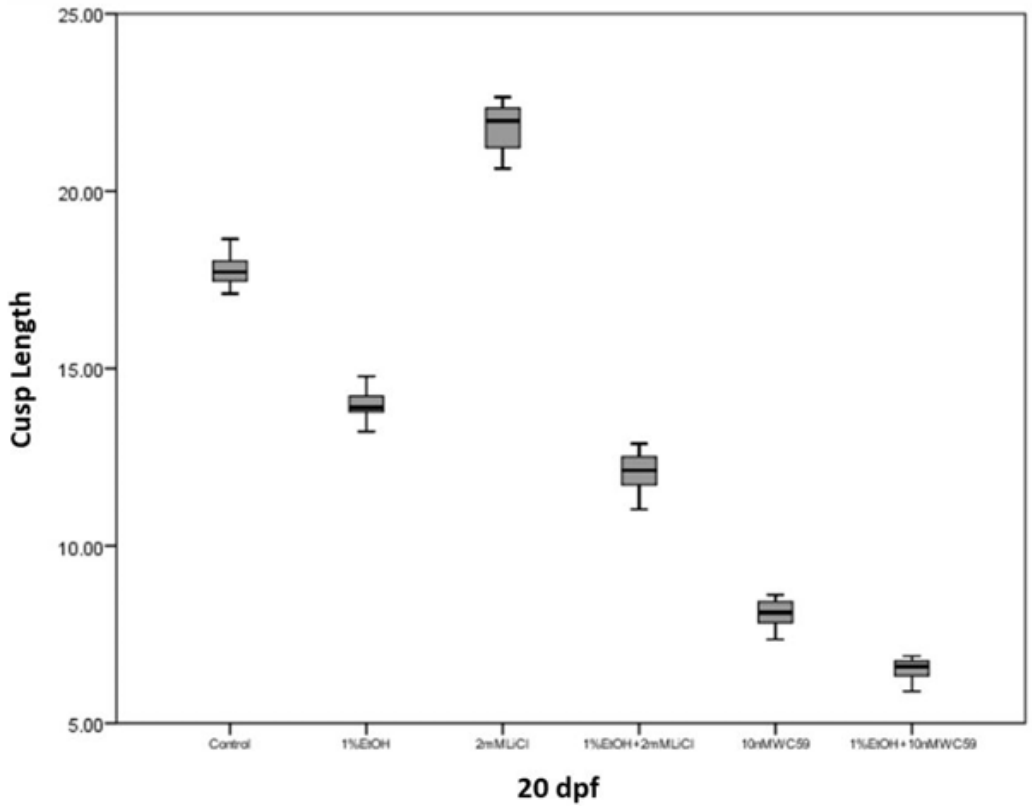

The Journal of Anatomy (ISSN 2995-6552)

**Supplemental Figure 8.** Comparing the cusp length between control and treated samples at 25 dpf. There was a significant difference in cusp length between the 2mMLiCl, 1%EtOH+2mMLiCl, 10nMWC59, and 1%EtOH+10nMWC59 treated groups with the control ($P < 0.05$), while there was no significant difference between 1%EtOH treated samples with the control ($P > 0.05$).

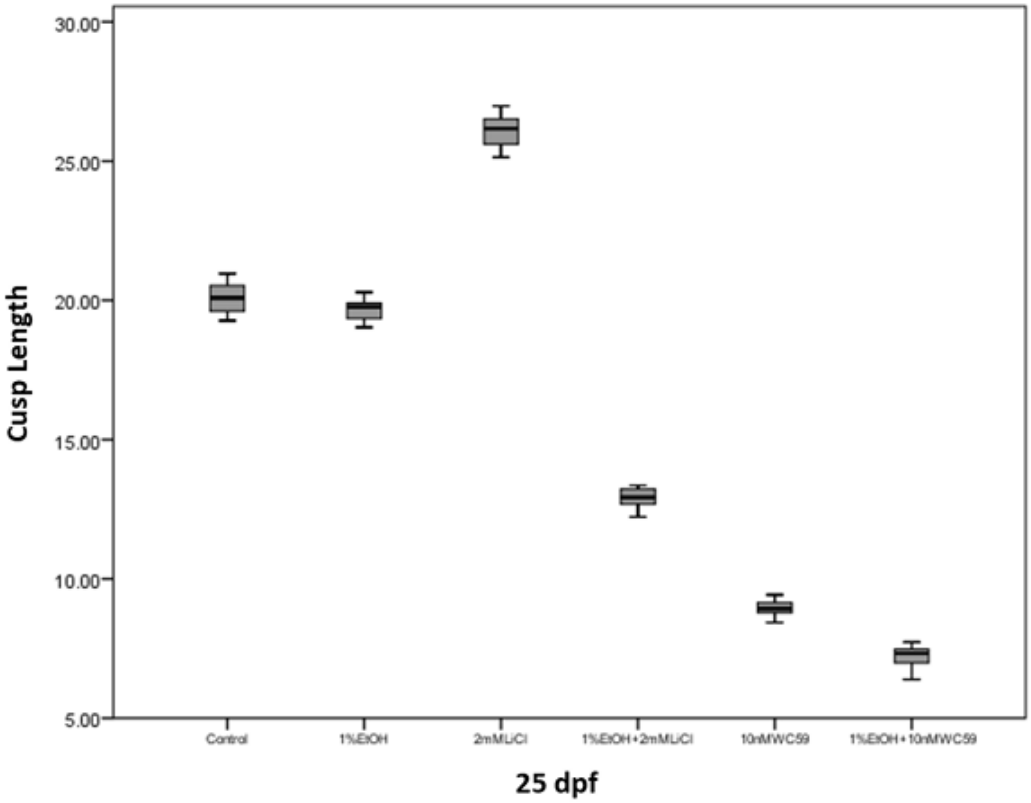


**Supplemental Figure 9.** Comparing the cusp length between control and treated samples at 30 dpf. There was a significant difference in cusp length between the 2mMLiCl, 1%EtOH+2mMLiCl, 10nMWC59, and 1%EtOH+10nMWC59 treated groups with the control ($P < 0.05$), while there was no significant difference between 1%EtOH treated samples with the control ($P > 0.05$).

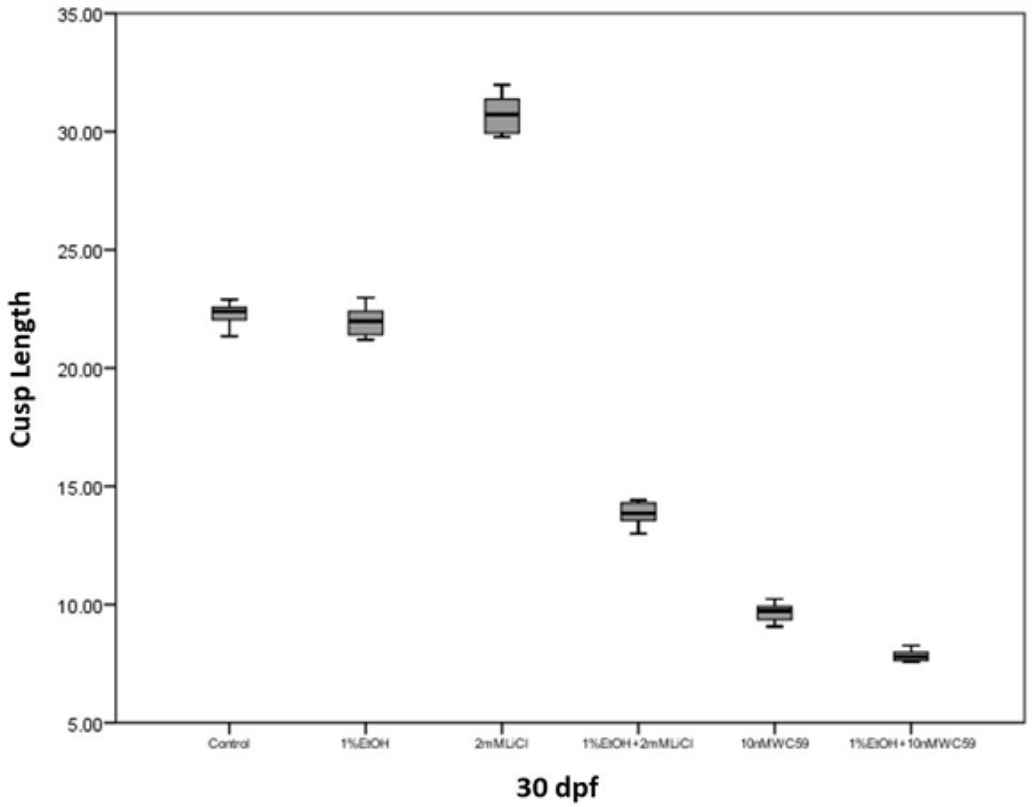

The Journal of Anatomy (ISSN 2995-6552)

## REFERENCES


1. Ten Cate's Oral Histology Development, Structure, and Function 9th Edition - August 15, 2017 Editor: Antonio Nanci Language: English eBook ISBN: 9780323485180

2. Almeida, L., V. Andreu-Fernández, E. Navarro-Tapia, R. Aras-López, M. Serra-Delgado, L. Martínez, O. García-Algar and M. D. Gómez-Roig (2020). "Murine Models for the Study of Fetal Alcohol Spectrum Disorders: An Overview." Front Pediatr 8: 359.

3. Atukorala, A. D. S. and R. K. Ratnayake (2021). "Cellular and molecular mechanisms in the development of a cleft lip and/or cleft palate; insights from zebrafish (Danio rerio)." Anat Rec (Hoboken) 304(8): 1650-1660.

4. Azimian Zavareh, P., P. Silva, N. Gimhani and D. Atukorallaya(2022)."EffectofEmbryonicAlcoholExposure on Craniofacial and Skin Melanocyte Development: Insights from Zebrafish (Danio rerio)." Toxics 10(9).

5. Barbazuk, W. B., I. Korf, C. Kadavi, J. Heyen, S. Tate, E. Wun, J. A. Bedell, J. D. McPherson and S. L. Johnson (2000). "The syntenic relationship of the zebrafish and human genomes." Genome Res 10(9): 1351-1358.

6. Barkley-Levenson, A. M. and J. C. Crabbe (2012). "Bridging Animal and Human Models: Translating From (and to) Animal Genetics." Alcohol Res 34(3): 325-335.

7. Blanck-Lubarsch, M., D. Dirksen, R. Feldmann, C. Sauerland and A. Hohoff (2019). "Tooth Malformations, DMFT Index, Speech Impairment and Oral Habits in Patients with Fetal Alcohol Syndrome." Int J Environ Res Public Health 16(22).

8. Bowden, D. M., P. S. Weathersbee, S. K. Clarren, C. E. Fahrenbruch, B. L. Goodlin and S. A. Caffery (1983). "A periodic dosing model of fetal alcohol syndrome in the pig-tailed macaque (Macaca nemestrina)." Am J Primatol 4(2): 143-157.

9. Church, M. W., F. Eldis, B. W. Blakley and E. V. Bawle (1997). "Hearing, language, speech, vestibular, and dentofacial disorders in fetal alcohol syndrome." Alcohol Clin Exp Res 21(2): 227-237.

10. Da Silva, K. and D. Wood (2021). "The oral health status and treatment needs of children with fetal alcohol spectrum disorder." Clin Oral Investig 25(6): 3497-3503.

11. Dangardt, F. and T. Chikritzhs (2020). "Is foetal alcohol syndrome in children as old as alcohol consumption?" Acta Paediatr 109(10): 1926-1927.

12. Dlugos, C. A. and R. A. Rabin (2003). "Ethanol effects on three strains of zebrafish: model system for genetic investigations." Pharmacology Biochemistry and Behavior 74(2): 471-480.

13. Eichler, A., J. Grunitz, J. Grimm, L. Walz, E. Raabe, T. W. Goecke, M. W. Beckmann, O. Kratz, H. Heinrich, G. H. Moll, P. A. Fasching and J. Kornhuber (2016). "Did you drink alcohol during pregnancy? Inaccuracy and discontinuity of women's self-reports: On the way to establish meconium ethyl glucuronide (EtG) as a biomarker for alcohol consumption during pregnancy." Alcohol 54: 39-44.

14. Erickson, T. and T. Nicolson (2015). "Identification of sensory hair-cell transcripts by thiouracil-tagging in zebrafish." BMC genomics 16(1): 1-10.

15. Fainsod, A. and G. Hicks (2018). "Special issue on fetal alcohol spectrum disorder." Biochem Cell Biol 96(2): v-vi.

16. Fernandes, Y., D. M. Buckley and J. K. Eberhart (2018). "Diving into the world of alcohol teratogenesis: a review of zebrafish models of fetal alcohol spectrum disorder." Biochem Cell Biol 96(2): 88-97.

17. Fraser, G. J., R. F. Bloomquist and J. T. Streelman (2013). "Common developmental pathways link tooth shape to regeneration." Dev Biol 377(2): 399-414.

18. Gupta, K. K., V. K. Gupta and T. Shirasaka (2016). "An Update on Fetal Alcohol Syndrome-Pathogenesis, Risks, and Treatment." Alcohol Clin Exp Res 40(8): 1594-1602.

19. Handrigan, G. R. and J. M. Richman (2010). "A network of Wnt, hedgehog and BMP signaling pathways regulates tooth replacement in snakes." Dev Biol 348(1): 130-141.

20. Huysseune, A. and J.-Y. Sire (1998). "Early development of the zebrafish (Danio rerio) pharyngeal dentition (Teleostei, Cyprinidae)." Anatomy and embryology 198(4): 289-305.

21. Huysseune, A. and J.-Y. Sire (2004). "The role of epithelial remodelling in tooth eruption in larval zebrafish." Cell and tissue research 315(1): 85-95.

22. Jackman, W. R., B. W. Draper and D. W. Stock (2004). "Fgf

signaling is required for zebrafish tooth development." Dev Biol 274(1): 139-157.

23. Jones, K. L., D. W. Smith, C. N. Ulleland and P. Streissguth (1973). "Pattern of malformation in offspring of chronic alcoholic mothers." Lancet 1(7815): 1267-1271.

24. Kitson, J. E., J. Ord and P. J. Watt (2022). "Maternal Chronic Ethanol Exposure Decreases Stress Responses in Zebrafish Offspring." Biomolecules 12(8).

25. Lemoine, P., H. Harousseau, J. P. Borteyru and J. C. Menuet (2003). "Children of alcoholic parents--observed anomalies: discussion of 127 cases." Ther Drug Monit 25(2): 132-136.

26. Lewis, K. E. and J. S. Eisen (2003). "From cells to circuits: development of the zebrafish spinal cord." Prog Neurobiol 69(6): 419-449.

27. Lim, W. H., B. Liu, D. Cheng, D. J. Hunter, Z. Zhong, D. M. Ramos, B. O. Williams, P. T. Sharpe, C. Bardet and S. j. Mah (2014). "Wnt signaling regulates pulp volume and dentin thickness." Journal of Bone and Mineral Research 29(4): 892-901.

28. Liu, F., E. Y. Chu, B. Watt, Y. Zhang, N. M. Gallant, T. Andl, S. H. Yang, M. M. Lu, S. Piccolo, R. Schmidt-Ullrich, M. M. Taketo, E. E. Morrisey, R. Atit, A. A. Dlugosz and S. E. Millar (2008). "Wnt/beta-catenin signaling directs multiple stages of tooth morphogenesis." Dev Biol 313(1): 210-224.

29. Lovely, C. B., Y. Fernandes and J. K. Eberhart (2016). "Fishing for Fetal Alcohol Spectrum Disorders: Zebrafish as a Model for Ethanol Teratogenesis." Zebrafish 13(5): 391-398.

30. Meyyazhagan, A., H. Kuchi Bhotla, V. Tsibizova, M. Pappuswamy, A. Chaudhary, V. A. Arumugam, M. Al Qasem and G. C. Di Renzo (2023). "Nutrition paves the way to environmental toxicants and influences fetal development during pregnancy." Best Pract Res Clin Obstet Gynaecol 89: 102351.

31. Mikkola, M. L. and S. E. Millar (2006). "The mammary bud as a skin appendage: unique and shared aspects of development." J Mammary Gland Biol Neoplasia 11(3-4): 187-203.

32. Nadiri, A., S. Kuchler-Bopp, Y. Haikel and H. Lesot (2004). "Immunolocalization of BMP-2/-4, FGF-4, and WNT10b in the developing mouse first lower molar." J Histochem Cytochem 52(1): 103-112.

33. Naidoo, S., G. Norval, S. Swanevelder and C. Lombard (2006). "Foetal alcohol syndrome: a dental and skeletal age analysis of patients and controls." Eur J Orthod 28(3): 247-253.

34. Ornoy, A. and Z. Ergaz (2010). "Alcohol abuse in pregnant women: effects on the fetus and newborn, mode of action and maternal treatment." Int J Environ Res Public Health 7(2): 364-379.

35. Parsons, K. J., A. Trent Taylor, K. E. Powder and R. C. Albertson (2014). "Wnt signalling underlies the evolution of new phenotypes and craniofacial variability in Lake Malawi cichlids." Nature communications 5(1): 1-11.

36. Raterman, S. T., J. R. Metz, F. Wagener and J. W. Von den Hoff (2020). "Zebrafish Models of Craniofacial Malformations: Interactions of Environmental Factors." Front Cell Dev Biol 8: 600926.

37. Reimers, M. J., M. E. Hahn and R. L. Tanguay (2004). "Two zebrafish alcohol dehydrogenases share common ancestry with mammalian class I, II, IV, and V alcohol dehydrogenase genes but have distinct functional characteristics." J Biol Chem 279(37): 38303-38312.

38. Ruiz-Heiland, G., S. Lenz, N. Bock and S. Ruf (2019). "Prevalence of WNT10A gene mutations in non-syndromic oligodontia." Clin Oral Investig 23(7): 3103-3113.

39. Sadeghi, F., J. S. Amoli, H. G. poor, M. Azarnia and T. Aliesfehani (2015). Modified double skeletal staining protocols with Alizarin red and Alcian blue in laboratory animals.

40. Sant' Anna, L., D. Tosello and M. Salgado (2005). "Histomorphometric study of the effects of ethanol on the enamel formation of rat mandibular molars during pregnancy." Braz Den J 22: 105-111.

41. Sant'Anna, L. B. and D. O. Tosello (2006). "Fetal alcohol syndrome and developing craniofacial and dental structures--a review." Orthod Craniofac Res 9(4): 172-185.

42. Sant'Anna, L. B., D. O. Tosello and S. Pasetto (2005). "Effects of maternal ethanol intake on immunoexpression of epidermal growth factor in developing rat mandibular molar." Arch Oral Biol 50(7): 625-634.

43. Sarkar, L. and P. T. Sharpe (1999). "Expression of Wnt signalling pathway genes during tooth development." Mech Dev 85(1-2): 197-200.

The Journal of Anatomy (ISSN 2995-6552)


44. Silva, P., P. Azimian Zavareh and D. Atukorallaya (2022). Teleost Fish as Model Animals to Understand Alcohol Teratology. Fetal Alcohol Spectrum Disorder: Advances in Research and Practice. A. E. Chudley and G. G. Hicks. New York, NY, Springer US: 31-48.

45. Sridharan, G. and A. A. Shankar (2012). "Toluidine blue: A review of its chemistry and clinical utility." J Oral Maxillofac Pathol 16(2): 251-255.

46. Tamura, M. and E. Nemoto (2016). "Role of the Wnt signaling molecules in the tooth." Jpn Dent Sci Rev 52(4): 75-83.

47. Thesleff, I. (2006). "The genetic basis of tooth development and dental defects." Am J Med Genet A 140(23): 2530-2535.

48. Thisse, B. and C. Thisse (2014). In situ hybridization on whole-mount zebrafish embryos and young larvae. In situ hybridization protocols, Springer: 53-67.

49. Vangipuram, S. D. and W. D. Lyman (2012). "Ethanol affects differentiation-related pathways and suppresses Wnt signaling protein expression in human neural stem cells." Alcohol Clin Exp Res 36(5): 788-797.

50. Vangipuram, S. D. and W. D. Lyman (2012). "Ethanol affects differentiation-related pathways and suppresses Wnt signaling protein expression in human neural stem cells." Alcoholism: Clinical and Experimental Research 36(5): 788-797.

51. Varatharasan, N., P. C. Croll and T. A. Franz-Odendaal (2009). "Taste bud development and patterning in sighted and blind morphs of Astyanax mexicanus." Developmental Dynamics 238(12): 3056–3064.

52. Vogel, P., R. Read, G. Hansen, D. Powell, P. Kantaputra, B. Zambrowicz and R. Brommage (2016). "Dentin dysplasia in Notum knockout mice." Veterinary pathology 53(4): 853-862.

53. Walker, M. B. and C. B. Kimmel (2007). "A two-color acid-free cartilage and bone stain for zebrafish larvae." Biotech Histochem 82(1): 23-28.

54. Whitehurst, T. (2010). Foetal alcohol spectrum disorders: the 21st century intellectual disability. Cognitive Impairments: causes,diagnosis and treatment. New York, Nova Science Publishers.

55. Xu, C. Q., S. M. de la Monte, M. Tong, C. K. Huang and M. Kim (2015). "Chronic Ethanol-Induced Impairment of Wnt/β-Catenin Signaling is Attenuated by PPAR-δ Agonist." Alcoholism: Clinical and Experimental Research 39(6): 969-979.

56. Yamashiro, T., L. Zheng, Y. Shitaku, M. Saito, T. Tsubakimoto, K. Takada, T. Takano-Yamamoto and I. Thesleff (2007). "Wnt10a regulates dentin sialophosphoprotein mRNA expression and possibly links odontoblast differentiation and tooth morphogenesis." Differentiation 75(5): 452-462.

57. Yang, J., S. K. Wang, M. Choi, B. M. Reid, Y. Hu, Y. L. Lee, C. R. Herzog, H. Kim-Berman, M. Lee, P. J. Benke, K. C. Lloyd, J. P. Simmer and J. C. Hu (2015). "Taurodontism, variations in tooth number, and misshapened crowns in Wnt10a null mice and human kindreds." Mol Genet Genomic Med 3(1): 40-58.

58. Yu, M., Y. Liu, Y. Wang, S. W. Wong, J. Wu, H. Liu, H. Feng and D. Han (2020). "Epithelial Wnt10a Is Essential for Tooth Root Furcation Morphogenesis." J Dent Res 99(3): 311-319.

59. Yuan, Q., M. Zhao, B. Tandon, L. Maili, X. Liu, A. Zhang, E. H. Baugh, T. Tran, R. M. Silva, J. T. Hecht, E. C. Swindell, D. S. Wagner and A. Letra (2017). "Role of WNT10A in failure of tooth development in humans and zebrafish." Mol Genet Genomic Med 5(6): 730-741.